Applied Mathematics & Information Sciences
An International Journal

http://dx.doi.org/10.12785/amis/090238

DOA Estimation for Arbitrary Four-Sensor Array Configurations based on Three-Dimensional Sound Intensity Measurement

*Jie Shi**

School of Marine Science and Technology, Northwestern Polytechnical University, 710072, Xi'an, China

Received: 9 Jun. 2014, Revised: 7 Sep. 2014, Accepted: 9 Sep. 2014
Published online: 1 Mar. 2015

Abstract: Vector sound intensity probe can be used to determine the DOA of a sound source by measuring the three orthogonal components of the sound-intensity vector. Typical vector sound intensity probes are composed of six or four sensors with symmetric structures. Such probes, in our opinion, are still not convenient for engineering implementation. A four-sensor vector sound intensity probe with arbitrary configurations is proposed here. The flexible structure of this probe allows it easily fix in any platform. In this paper, the direction finding algorithm based on this four-sensor probe is investigated first, then the error in direction estimates caused by instrument systematic error in sound intensity measurements are analyzed theoretically. Last, simulation experiments are conducted for testing the performance of DOA estimation based on this probe.

Keywords: vector sound intensity probe; sound intensity measurement,direction-of-arrival(DOA) estimation,four-sensor, arbitrary configuration,error analysis

1 Introduction

Sound intensity in its vector form became routinely measurable since 1980s with the development of two-channel analyzers and the discovery of the cross-spectral formulation [1,2] of the components of the sound-intensity vector. In practice most sound-intensity measurements are made using a probe consisting of two sensors to determine the component of sound intensity perpendicular to a given measurement surface. Mathematically sound intensity is expressed as the product of acoustical pressure and velocity, where pressure is the arithmetic mean of the pressures measured by sensor pair and velocity is derived from the pressure difference [3]. Therefore, the sound intensity is

$$I_r = \lim_{T\to\infty} \frac{1}{T} \int_{-\frac{T}{2}}^{\frac{T}{2}} \frac{p_1(t)+p_2(t)}{2} \left[-\frac{1}{\rho} \int \frac{p_1(t)-p_2(t)}{d} dt \right] dt \quad (1)$$

Where I_r is the instantaneous intensity along the line connecting the sensor pair, p_1 and p_2 are the acoustical pressures measured by sensor pair, d is the separation between the acoustic centers of the pressure sensors, and ρ is mass density of the fluid. Fahy[4] and Chung[5] modified this equation with the help of Fourier transforms to develop an expression suitable for digital signal processing. In the frequency domain, it is given by

$$I(f) = -\mathrm{Im}\frac{P_1^*(f)P_2(f)}{2\pi f \rho d} \quad (2)$$

Where Im[] indicates the imaginary part, $P_1(f)$ and $P_2(f)$ are the Fourier-transformed two sensor sound pressure signals. The symbol * represents complex conjugation, f is the frequency in Hz. Since 1990s, a few papers [6,7] have described four- or six-sensor probes that simultaneously measure all three components of the sound-intensity vector. The six-sensor vector sound intensity probe[8] is composed of three pairs of sensors with pairs aligned along orthogonal axes as shown in figure 1. Each sensor pair provides one of the components of the three dimensional intensity vectors I_x, I_y and I_z. Where I_x, I_y and I_z also define the x, y and z Cartesian components. The four-transducer probe[9] is composed of four sensors with sensors at each of vertices of a regular tetrahedron as shown in figure 2. With this arrangement, pressures measured at the four vertices are averaged in

* Corresponding author e-mail: shijienpu@nwpu.edu.cn

pairs to give a finite-difference approximation of the pressure at each of the six midpoints of the edges of the tetrahedron. The four-sensor vector sound intensity probe can also measure the three orthogonal components of sound intensity at the center of the tetrahedron.

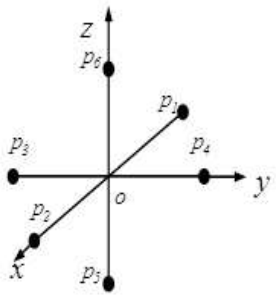

Fig. 1: Six-sensor vector sound intensity probe

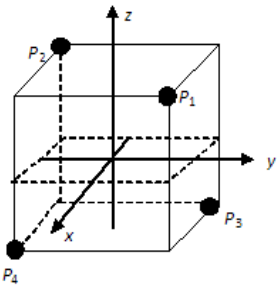

Fig. 2: Four-sensor vector sound intensity probe

The three components I_x, I_y and I_z of the sound intensity vector can be used to find the direction of a sound source using azimuth (horizontal) and elevation (vertical) angles θ and ϕ.

$$\tan\phi = \frac{I_y}{I_x} \quad \cos\theta = \frac{I_z}{I} \tag{3}$$

Where sound intensity $I = \sqrt{I_x^2 + I_y^2 + I_z^2}$. It should be noted that the signs of the different components of the sound intensity vector provide the information needed to avoid 180 deg ambiguities. Therefore, the vector sound intensity probes can not only measure sound intensity vector, but also find the direction of sound sources. And the main advantage of these vector probes over traditional scalar sensors is that they allow the use of fewer sensors and smaller array apertures, while maintaining performance. This character makes vector sound intensity probes very useful for locating a low-frequency underwater sound source, while a traditional linear additive array of pressure sensors is too large to be fix in smaller facilities[8,10,11]. Two-dimensional acoustic vector sensors have been used in several Navy systems, like the DIFAR sonobuoy and the AN/WLR-9 acoustic intercept receiver [12] . These devices have made important contributions to the Navy sonar community, where it is desirable to obtain an accurate DOA estimation or bearing to a low-frequency target from a single point in space. But the changeless structure sometimes restricts its application. This paper proposes a four-sensor vector sound intensity probe with arbitrary configurations which has more flexible configuration than the typical six- and four-sensor vector sound intensity probe shown in figure 1 and figure 2. We investigate the direction estimation algorithm based on this four-sensor probe and analyze theoretically the error in direction estimation caused by instrument systematic errors. And we examine two examples of the application of probes with arbitrary configurations to DOA estimation of an underwater sound source by simulating.

2 DOA Estimation for Arbitrary Four-Sensor Array Configurations

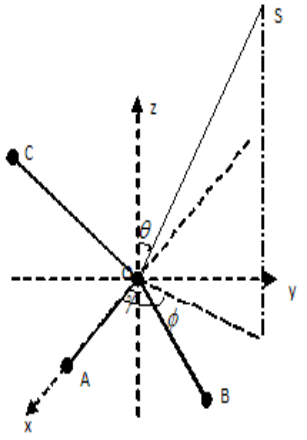

Fig. 3: A four-sensor vector sound intensity probe with arbitrary geometry

As shown in figure 3, four sensors are arranged arbitrarily but not in a same plane. The four sensors are assumed to be located at points *O*, *A*, *B* and *C*. Where point *O* is selected as origin of Cartier Coordinate System and points *O*, *A*, *B* can form a plane which is selected as *xoy* plane. The coordinates of points *O*, *A*, *B* and *C* are (0,0,0), (x_a,0,0) , (x_b, y_b, 0) and (x_c, y_c, z_c) respectively. Where x_a,x_b,y_b,x_c, y_c and z_c are all known. d_{OA}, d_{OB} and d_{OC} are the distances from sensors at point *O* to points *A*, *B* ,*C*, respectively. And they are all restricted by $kd << 1$, where k is the wave number. $\gamma$is the angle between vectors **OA** and **OB**, and it can be expressed as $\gamma = \tan^{-1}\frac{y_b}{x_b}$.

I_{OA}, I_{OB} and I_{OC} are the components of the sound intensity **I** caused by sound source *S* along the directions

of vectors **OA**,**OB** and **OC** The instantaneous sound intensity components can be calculated by (1) and expressed as:

$$I_{OA} = \lim_{T\to\infty} \frac{1}{T} \int_{-\frac{T}{2}}^{\frac{T}{2}} \frac{p_O(t)+p_A(t)}{2} \left[-\frac{1}{\rho} \int \frac{p_O(t)-p_A(t)}{d} dt \right] dt$$
$$I_{OB} = \lim_{T\to\infty} \frac{1}{T} \int_{-\frac{T}{2}}^{\frac{T}{2}} \frac{p_O(t)+p_B(t)}{2} \left[-\frac{1}{\rho} \int \frac{p_O(t)-p_B(t)}{d} dt \right] dt$$
$$I_{OC} = \lim_{T\to\infty} \frac{1}{T} \int_{-\frac{T}{2}}^{\frac{T}{2}} \frac{p_O(t)+p_C(t)}{2} \left[-\frac{1}{\rho} \int \frac{p_O(t)-p_C(t)}{d} dt \right] dt \quad (4)$$

Where $p_O(t)$, $p_A(t)$, $p_B(t)$ and $p_C(t)$ are the acoustical pressures measured by sound pressure sensor located at points *O*, *A*, *B* and *C*. According to cross-spectral formulation, the frequency domain of the sound intensity components can be calculated by equation (2) and expressed as

$$I_{OA}(f) = -\frac{1}{2\pi f \rho d_{OA}} \mathrm{Im}\left[S_{OA}(f)\right]$$
$$I_{OB}(f) = -\frac{1}{2\pi f \rho d_{OB}} \mathrm{Im}\left[S_{OB}(f)\right] \quad (5)$$
$$I_{OC}(f) = -\frac{1}{2\pi f \rho d_{OC}} \mathrm{Im}\left[S_{OC}(f)\right]$$

Where, $\mathrm{Im}[S_{OA}(f)]$, $\mathrm{Im}[S_{OB}(f)]$ and $\mathrm{Im}[S_{OC}(f)]$ are the imaginary part of the cross spectrum of the pressures received at point *O* and *A*,*B*,*C*. To find the direction of sound source *S*, the three orthogonal components of sound intensity vector must be known. Then how to measure the three orthogonal components I_x, I_y and I_z by the four-sensor vector sound intensity probe is the key point. From the arrangement of the four sensors shown in figure 3, we can deduce the relation between I_{OA}, I_{OB} and I_{xoy} . I_{xoy} is the projection of the sound intensity vector on the *xoy* plane.

$$I_{OA} = I_{xoy}\cos\phi \quad (6)$$

$$I_{OB} = I_{xoy}\cos(\gamma-\phi) \quad (7)$$

The direction of vector **OA** is the direction of *x*-axis, so I_{OA} is the *x*-component of sound intensity vector.

$$I_x = I_{OA} \quad (8)$$

Then the *y*-component of the sound intensity vector can be expressed as

$$I_y = I_{xoy}\sin\phi = \frac{I_{OB} - I_{OA}\cos\gamma}{\sin\gamma} \quad (9)$$

Where I_{OA}, I_{OB} and γ are known qualities, and the numerator $\sin\gamma \neq 0$. Sound intensity **I** can be written as $\mathbf{I} = (I_x, I_y, I_z)$, the dot product of **I** and $\mathbf{I_{OC}}$ results in a scalar can be given by

$$\mathbf{I}\cdot\mathbf{I_{OC}} = x_c I_x + y_c I_y + z_c I_z \quad (10)$$

So the *z*-component of vector **I** can be expressed as

$$I_z = \frac{d_{OC} I_{OC} - x_c I_{OA} - y_c (I_{OB} - I_{OA}\cos\gamma)/\sin\gamma}{z_c} \quad (11)$$

Now the three orthogonal components I_x, I_y and I_z can be calculated by equation (8) (9)and (11),respectively. then the azimuthal angle ϕ and elevation angle θ can be obtained by equation (3). Figure 4 shows two types of vector sound intensity probe maybe fix in some platforms in real engineering implementation. The configuration of four sensors of the probe can be arbitrarily arranged to adjust the form of instruments.

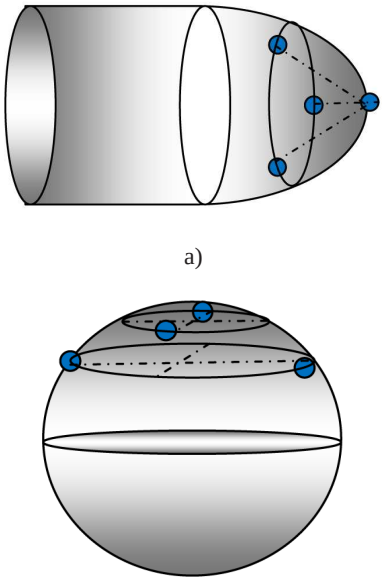

a)

b)

Fig. 4: two type vector sound intensity arrays fix on platforms

3 Analysis of direction estimation error

Many factors, namely, finite difference approximation for calculation, the phase mismatch between the measuring channels, the directional characteristics of the probe itself, the presence of holding devices and the conditions of the actual sound field will influence the accuracy of sound measurement, and also influence the accuracy of direction sensing. All measurement errors can be divided into two types: bias errors and random errors[13]. Random errors reveal themselves by poor repeatability and reproducibility, therefore it can always be recommended to repeat the measurement to reduce the random error in practice. The detailed analysis of the random error in sound intensity measurement and

direction estimates are given by Thierry [14]. Bias errors are more subtle, no amount of averaging will reduce such errors. According to Fahy [4], systematic error is the distinct source of bias error which occur when estimating sound intensity using vector sound intensity probe. Most important sources of system error are: (a) the finite-difference approximations(FDAE), (b) phase-mismatch error and imbalance between the sensor channels(IPME). In this section the direction estimation error caused by systematic error in sound intensity measurement is deduced based on two assumptions: a) the vector sound intensity probe is located in the far-field of the sound source, b) the sound field is a harmonic sound filed. Here, the finite-difference approximation error and phase-mismatch error are discussed together. For a harmonic sound field of frequency, w, the (real) acoustic pressure received at *O*, *A*, *B* and *C* are given as:

$$\begin{aligned} p_O &= P_0 e^{j(wt-kr_0)} \\ p_A &= P_0 e^{j[wt-k(r_0-d_{OA}\cos\alpha_{OA})]} \\ p_B &= P_0 e^{j[wt-k(r_0-d_{OB}\cos\alpha_{OB})]} \\ p_C &= P_0 e^{j[wt-k(r_0-d_{OC}\cos\alpha_{OC})]} \end{aligned} \tag{12}$$

Where P_0 is the pressure amplitude, k is wave number, $r_0$is the distance between the sound source and the origin O. α_{OA}, α_{OB}, α_{OC} are the angles of directions for the incident plane wave of sound source with respect to the vectors **OA**, **OB** and **OC** respectively. The relation between α and direction of the sound source (ϕ,θ) is

$$\begin{aligned} \cos\alpha_{OA} &= \sin\theta\cos\phi \\ \cos\alpha_{OB} &= \frac{x_b\sin\theta\cos\phi + y_b\sin\theta\sin\phi}{d_{OB}} \\ \cos\alpha_{OC} &= \frac{x_c\sin\theta\cos\phi + y_c\sin\theta\sin\phi + z_c\cos\theta}{d_{OC}} \end{aligned} \tag{13}$$

Then the three components of sound intensity along the directions of **OA**, **OB** and **OC** can be achieved by cross-spectrum formulation expressed by equation (2) :

$$\begin{aligned} \hat{I}_{OA} &= \frac{p_0^2\sin(kd_{OA}\cos\alpha_{OA}+\Delta\varphi_{OA})}{2\pi f\rho d_{OA}} \\ \hat{I}_{OB} &= \frac{p_0^2\sin(kd_{OB}\cos\alpha_{OB}+\Delta\varphi_{OB})}{2\pi f\rho d_{OB}} \\ \hat{I}_{OC} &= \frac{p_0^2\sin(kd_{OC}\cos\alpha_{OC}+\Delta\varphi_{OC})}{2\pi f\rho d_{OC}} \end{aligned} \tag{14}$$

Where $\Delta\varphi_{OA}$, $\Delta\varphi_{OB}$ and $\Delta\varphi_{OC}$ are the instrument phase difference between sensor at point O and sensors at point A,B and C, respectively. The three orthogonal components of sound intensity can be calculated by substitution equation (14)into equations (8),(9) and (11).

$$\begin{aligned} \hat{I}_x &= \hat{I}_{OA} = \frac{p_0^2\sin(kd_{OA}\cos\alpha_{OA}+\Delta\varphi_{OA})}{2\pi f\rho d_{OA}} \\ \hat{I}_y &= \frac{\hat{I}_{OB}-\hat{I}_{OA}\cos\gamma}{\sin\gamma} = \frac{p_0^2\sin(kd_{OB}\cos\alpha_{OB}+\Delta\varphi_{OB})}{2\pi f\rho d_{OB}\sin\gamma} \\ &- \frac{p_0^2\cos\gamma\sin(kd_{OA}\cos\alpha_{OA}+\Delta\varphi_{OA})}{2\pi f\rho d_{OA}\sin\gamma} \\ \hat{I}_z &= \frac{d_{OC}}{z_c}\hat{I}_{OC} - \frac{x_c}{z_c}\hat{I}_{OA} - \frac{y_c}{z_c\sin\gamma}(\hat{I}_{OB}-\hat{I}_{OA}\cos\gamma) \\ &= \frac{p_0^2 sin(kd_{OC}\cos\alpha_{OC}+\Delta\varphi_{OC})}{2\pi f\rho z_c} \\ &- \frac{p_0^2 y_c sin(kd_{OB}\cos\alpha_{OB}+\Delta\varphi_{OB})}{2\pi f\rho d_{OB} z_c\sin\gamma} \\ &+ \frac{p_0^2(y_c\cos\gamma - x_c\sin\gamma)\sin(kd_{OA}\cos\alpha_{OA}+\Delta\varphi_{OA})}{2\pi f\rho d_{OA} z_c\sin\gamma} \end{aligned} \tag{15}$$

The (real) sound intensity of a plane wave which was determined from acoustical pressure, using the so-called far-field approximation[15,16] can be expressed as $I \approx p_0^2/\rho c$. Compare to the real sound intensity components with estimated ones expressed by equation (15), the ratio between the estimated value and the real value can be expressed as

$$\begin{aligned} m_x &= \frac{\hat{I}_x}{I_x} = \frac{\hat{I}_x}{I\sin\theta\cos\phi} = \frac{\sin(kd_{OA}\cos\alpha_{OA}+\Delta\varphi_{OA})}{kd_{OA}\cos\alpha_{OA}} \\ m_y &= \frac{\hat{I}_y}{I_y} = \frac{\hat{I}_y}{I\sin\theta\sin\phi} = \frac{sin(kd_{OB}\cos\alpha_{OB}+\Delta\varphi_{OB})}{kd_{OB}\sin\gamma\sin\theta\sin\phi} \\ &- \frac{\cos\gamma\sin(kd_{OA}\cos\alpha_{OA}+\Delta\varphi_{OA})}{kd_{OA}\sin\gamma\sin\theta\sin\phi} \\ m_z &= \frac{\hat{I}_z}{I_z} = \frac{\hat{I}_z}{I\cos\theta} \\ &= \frac{x_c\sin[k(x_c\sin\theta\cos\phi + y_c\sin\theta\sin\phi + z_c\cos\theta)+\Delta\varphi_{OC}]}{kz_c\cos\theta} \\ &- \frac{y_c}{z_c\sin\gamma}\frac{\sin[k(x_b+y_b)\sin\theta\cos\phi+\Delta\varphi_{OB}]}{kd_{OB}\cos\theta} \\ &+ \frac{(y_c\cos\gamma - x_c\sin\gamma)}{z_c\sin\gamma}\frac{sin(kd_{OA}\sin\theta\cos\phi+\Delta\varphi_{OA})}{kd_{OA}\cos\theta} \end{aligned} \tag{16}$$

So, error in elevation angle and azimuth angle estimates caused by the finite-difference approximation and phase-mismatch can be shown as

$$\begin{aligned} \Delta\theta &= \frac{\partial\theta}{\partial I_x}\Delta I_x + \frac{\partial\theta}{\partial I_y}\Delta I_y + \frac{\partial\theta}{\partial I_z}\Delta I_z \\ &= (m_x-1)\cos\theta\cos\phi\sin\theta\cos\phi + (m_y-1) \\ &\cos\theta\sin\phi\sin\theta\sin\phi - (mz-1)\sin\theta\cos\theta \\ \Delta\phi &= \frac{\partial\phi}{\partial I_x}\Delta I_x + \frac{\partial\phi}{\partial I_y}\Delta I_y = (m_y-m_x)\sin\theta\cos\phi \end{aligned} \tag{17}$$

In equations (16) and (17), the error in DOA estimates due to finite-difference approximation in sound intensity measurements can be achieved by setting the phase mismatch between probe channels to zeros, i.e. $\Delta\varphi_{OA} = \Delta\varphi_{OB} = \Delta\varphi_{OC} = 0$. And the error due to phase mismatch can be achieved by assuming $\sin x \approx x, x \leq 1$. Here we chose a typical orthogonal four-sensor vector sound intensity probe for an example to calculate the direction error caused by FDAE and IPME by equations (**??**) and (**??**) . We assume that the coordinates of the four sensor points *O*, *A*, *B* and *C* are (0,0,0), (*d*,0,0) , (0, *d*, 0) and (0,0,*d*), and $\Delta\varphi_{OA} = \Delta\varphi_{OB} = \Delta\varphi_{OC} = 0.5^\circ$. The sound source is located at $\theta = 60^\circ$ and $\phi = 80^\circ$ relative to the probe. Figure 5 shows the direction measurement errors due to FDAE and IPME with the varying kd. The simulation results show that error due to FDAE increases when *kd* is increasing, while error due to IPME decreases. This conclusion is consistent with the error in sound intensity measurement by vector sound intensity probe[17].

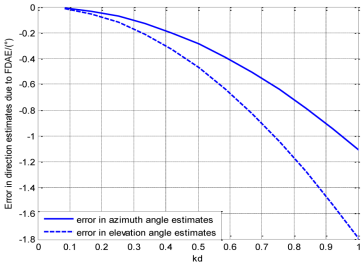

a)

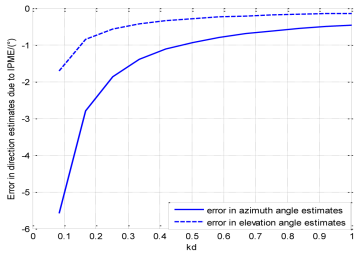

b)

Fig. 5: Error in direction estimates caused by FDAE and IPME in sound intensity measurement.a) Error caused by FDAE;b)Error caused by IPME.

4 Numerical results

In this section we will examine some examples of the application of four-sensor arrays with arbitrary configurations to the estimation of DOA of an underwater sound source by simulating. Here we consider the ocean ambient noise is an isotropic noise field, which is made up of statistically independent waves arriving from all possible angles and is similar to the models described by Cron and Sherman[18]. We assume a monopole source in free field is located on a circle with elevation angle θ=60° andθ=30° relative to the probe, and the azimuth angle is changed from $\phi = 0$ to 360 deg with steps of 10 deg. The I_x, I_y and I_z components of the sound intensity vector are calculated at each step by using the formula in equations (8) ,(9) and (11), and the angleθ and ϕ are determined using the formula in (3). For reducing the random error in DOA estimates due to ambient noise, each spectrum of the intensity components, I_x, I_y and I_z is consisting of sixty spectral averages. The phase differences between sensors of the probe are $\Delta\varphi_{OA} = \Delta\varphi_{OB} = \Delta\varphi_{OC} = 0.5^\circ$.The sound source radiated harmonic signal with frequency f=800Hz and signal to noise ratio is 10dB.

A.Direction finding with the four-sensor probe shown in figure 4a)

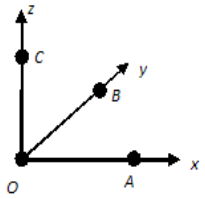

We redraw the configuration of the probe shown in fig.4a) as the left figure. Typically we assume that the coordinates of the four sensors of the probe are *O*(0,0,0), *A*(0.2,0,0), *B* (0, 0.2, 0) and *C*(0,0,0.2). That is, **OA**, **OB** and **OC** are orthogonal to each other and their length are all equal to 0.2m. The results of direction finding are shown in figure 6 and 7. After averaging to reduce error due to ambient noise, the errors in angle estimates are within 2°.

B. Direction finding with the four-sensor probe shown in figure 4b)

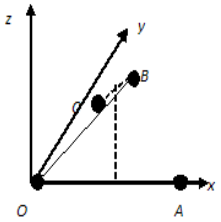

A four-sensor vector sound intensity probe can be fixed in a platform as shown in fig.4b). For finding DOA of a sound source by this probe, we must put these four sensors in Cartier coordinate system so that we can calculating three orthogonal components of sound intensity vector. As shown in the left figure, sensor *O* is put on the origin of the coordinate, sensor *A* is on the *x*-axis. The length of **OA** is assumed to be 0.2m. Vector **OB** and **OA** are designed to be orthogonal, and the distance between them is set to be 0.2m. The length of *vecBC* is 0.1m. The results of direction finding are shown in figure 10 and 11. The results show that the errors in angle estimates are within in 3°.

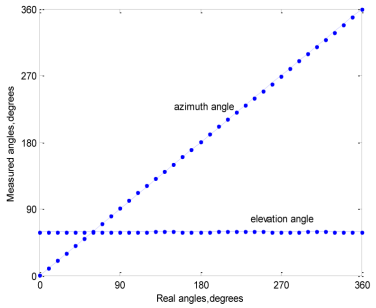

a)

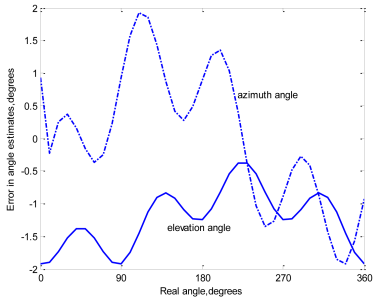

b)

Fig. 6: Elevation angle θ=60° a) Comparison of measured angles with real settings. b) Error in angle estimates.

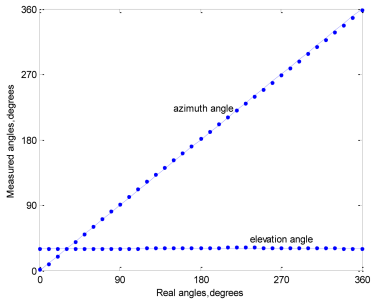

a)

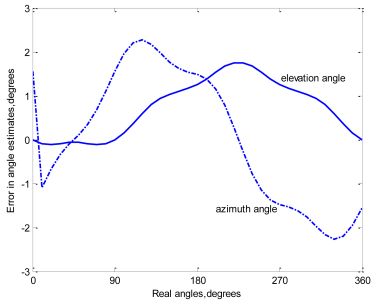

b)

Fig. 8: Elevation angle θ=60° a) Comparison of measured angles with real settings. b) Error in angle estimates.

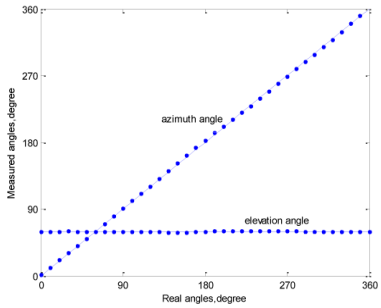

a)

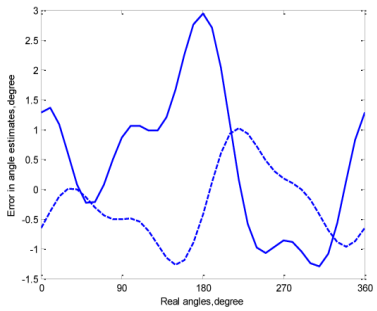

b)

Fig. 7: Elevation angle θ=30° a) Comparison of measured angles with real settings. b) Error in angle estimates.

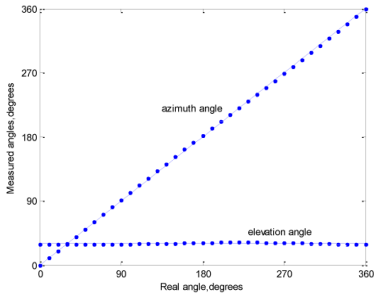

a)

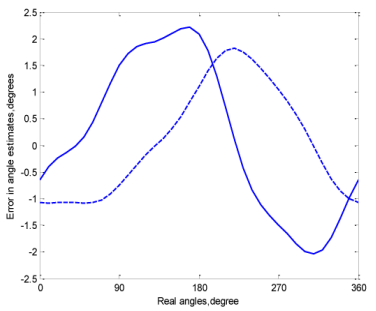

b)

Fig. 9: Elevation angle θ=30° a) Comparison of measured angles with real settings. b) Error in angle estimates.

5 Conclusion

In this paper, we considered the DOA estimation for arbitrary Compared to the symmetric arrangement of pressure sensors of vector sound intensity probes, the arbitrary configuration of four- sensor probe, appears to provide an unrestricted structure in engineering implementation. DOA estimation via the vector sound intensity probe we proposed here is still based on three orthogonal components of sound intensity measurements.

References

[1] J.Y Chung, Cross-spectral method of measuring acoustic intensity, Research Publication, No. GMR-2617 General Motors Research Laboratories, Warren, MI, (1977).

[2] F.J Fahy,Sound Intensify. London: Elsevier, (1989).

[3] J.A Mann,J.Tichy and A.J Romana. Instantaneous and time averaged energy transfer in acoustic fields,Journal of Acoustic Society of America **82**, 17-80 (1987).

[4] F.J Fahy, Measurement of acoustic intensity using the cross-spectral density of two microphone signals, Journal of Acoustic Society of America **62**, 1057-1059 (1977).

[5] J.Y Chung, Cross-spectral method of measuring acoustic intensity without error caused by instrument phase mismatch, Journal of Acoustic Society of America **64**, 1613-1616 (1978).

[6] G.Rasmussen, Measurement of vector fields. Proceedings of the Second International,Congress on Acoustic Intensity, CETIM, Senlis, France, 52-58 (1985).

[7] L.Mantors,C.C Rodrigues, and J.L Nento Coelho,Measuring the three dimension acoustic intensity vector with a four-microphone probe, Proceedings INTER-NOISE, 965-968 (1989).

[8] D.Hutt, P.C Hinwa,A.A.J Hamilton, Measurement of Underwater Sound Intensity Vector, **2**, 717-722 (1999).

[9] R.Hickling,W.Wei and R.Raspet, Finding the direction of a sound source using a vector sound-intensity probe. Journal of Acoustic Society of America **94**, 2408-2412 (1993).

[10] R.Hickling,W.Wei, Use of pitch-azimuth plots in determining the direction of a noise source in water with a vector sound-intensity probe, Journal of Acoustic Society of America **94**, 856-866 (1995).

[11] R.Hickling,Locating sound sources with vector sound-intensity probes, using polynomial continuation, Journal of Acoustic Society of America **100**, 49-56 (1996).

[12] M.T Silvia, R.T Richards,A theoretical and experimental investigation of low-frequency acoustic vector sensors, Proceeding of OCEANS **3**, 112-118 (2002).

[13] F.Jacobsen,An Overview of the Sources of Error in Sound Power Determination Using the Intensity Technique,Applied Aoustics **50**, 155-166 (1997).

[14] T.Loyau,Statistical errors in the estimation of the magnitude and direction of the complex acoustic intensity vector,Journal of Acoustic Society of America **97**, 2952-2962 (1995).

[15] U.S Shirahatti, Two-microphone finite difference approximation errors in the interference fields of poing dipole sources, Journal of Acoustic Society of America **92**, 250-267 (1992).

[16] A.D Pierce,An introduction to its physical principles and applications, AIP, New York, 39-42 (1989).

[17] M.L Munhal,An error inherent in the use of the two-microphone method for gas pulsation measurement in a reflective environment,Journal of Sound and Vibration **242**, 539-541 (2001).

[18] B.F Cron and C.H Sherman, Spatial-correlation functions fro various noise models, Journal of Acoustic Society of America **34**, 1732-1736 (1962).

Jie Shi received the PhD degree in Communication and Information System at Northwestern Polytechnical University. Her research interests are in the areas of sonar signal processing including the underwater ambient noise models, direction or localization estimation, signal detection.